Synthesis, X-ray Analysis, and Biological Evaluation of a New Class of Stereopure Lactam-Based HIV-1 Protease Inhibitors

Xiongyu Wu,[†] Per Öhrngren,[†] Advait A. Joshi,[†] Alejandro Trejos,[†] Magnus Persson,[‡] Riina K. Arvela,[†] Hans Wallberg,[§] Lotta Vrang,[§] Åsa Rosenquist,[§] Bertil B. Samuelsson,[§] Johan Unge,[∥] and Mats Larhed*,[†]

[†]Department of Medicinal Chemistry, Organic Pharmaceutical Chemistry, BMC, Uppsala University, P.O. Box 574, SE-751 23 Uppsala, Sweden

[‡]Department of Cell and Molecular Biology, Structural Biology, BMC, Uppsala University, P.O. Box 596, SE-751 24 Uppsala, Sweden

[§]Medivir AB, P.O. Box 1086, SE-141 22 Huddinge, Sweden

[∥]MAX IV-Laboratory, Lund University, P.O. Box 118, SE-221 00 Lund, Sweden

Ⓢ *Supporting Information*

ABSTRACT: In an effort to identify a new class of druglike HIV-1 protease inhibitors, four different stereopure β-hydroxy γ-lactam-containing inhibitors have been synthesized, biologically evaluated, and cocrystallized. The impact of the tether length of the central spacer (two or three carbons) was also investigated. A compound with a shorter tether and (3R,4S) absolute configuration exhibited high activity with a K_i of 2.1 nM and an EC_{50} of 0.64 μM. Further optimization by decoration of the P1′ side chain furnished an even more potent HIV-1 protease inhibitor (K_i = 0.8 nM, EC_{50} = 0.04 μM). According to X-ray analysis, the new class of inhibitors did not fully succeed in forming two symmetric hydrogen bonds to the catalytic aspartates. The crystal structures of the complexes further explain the difference in potency between the shorter inhibitors (two-carbon spacer) and the longer inhibitors (three-carbon spacer).
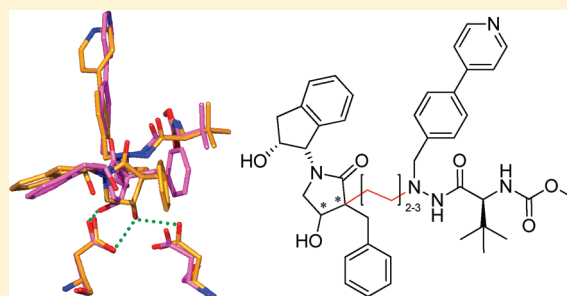
INTRODUCTION

More than 25 years after the identification of the causative agent of AIDS,[1,2] HIV/AIDS is still a major challenge to society. The latest WHO/UNAIDS report (2010) states that the number of people living with HIV has risen to 33.3 million, with more than 2.6 million new cases annually and almost 5000 AIDS-related deaths per day.[3]

With the introduction of the first HIV-1 protease inhibitor (PI) (saquinavir[4]) in 1995 and the development of highly active antiviral therapy (HAART)[5−7] the clinical outcome of HIV/ AIDS changed from a lethal to a manageable, but chronic, disease in the developed world.[8−10] The early PIs suffered from poor pharmacokinetic profiles and caused severe side effects such as hepatic toxicity and lipodystrophy.[11,12] For these reasons and with a frequent daily dosing regimen, they were not the first-hand choice in HAART. The most common combinations in early HAART were instead two nucleoside reverse transcriptase inhibitors (NRTIs) together with a non-nucleoside reverse transcriptase inhibitor (NNRTI). The development of NNRTI- and/or NRTI-resistant HIV strains and the introduction of new PIs, with a once-daily dose regime and improved effect profiles, have made the combination of a PI together with two NRTIs a more frequent choice for first line treatment in HAART.[8,13,14]

Although saquinavir has, to date, been followed by eight other PIs (ritonavir, indinavir, fosamprenavir, nelfinavir, lopinavir, atazanavir, tipranavir, and darunavir),[15] improving pharmacokinetic properties and reducing adverse effects are still issues that need to be addressed.[16−18] Further, the rapid replication and the high mutation rate of the HIV-1 virus,[19,20] together with the mutation pressure induced by today's pharmacotherapies, will lead to an increase in the problems associated with resistant virus strains. Thus, we cannot expect the good results currently seen with HAART to continue if new drugs are not developed and introduced onto the market.[17,21]

We have been engaged in the development of novel HIV-1 PIs since 1997.[22] In our most recent program we developed novel classes of potent HIV-1 PIs incorporating a shielded tertiary alcohol as part of the transition state mimic.[23−28] Inspired by the structure of the potent inhibitor Atazanavir (ATZ)[29,30] (Figure 1), we used a similar hydrazide moiety in the prime side[31] of our new *tert*-hydroxy-containing PIs. By altering the length of the central backbone, using a one-, two-, or three-carbon spacer (Figure 1, series **A**,[23−25] **B**,[26] and **C**,[27,28] respectively), we focused on optimizing the interaction with the catalytically active aspartic acid residues of the enzyme.

The prepared *tert*-hydroxy comprising PIs rendered good affinity and potency.[23−28] Class **B**, with the two-carbon spacer, yielded the best results, with values of K_i and EC_{50} as low as 1
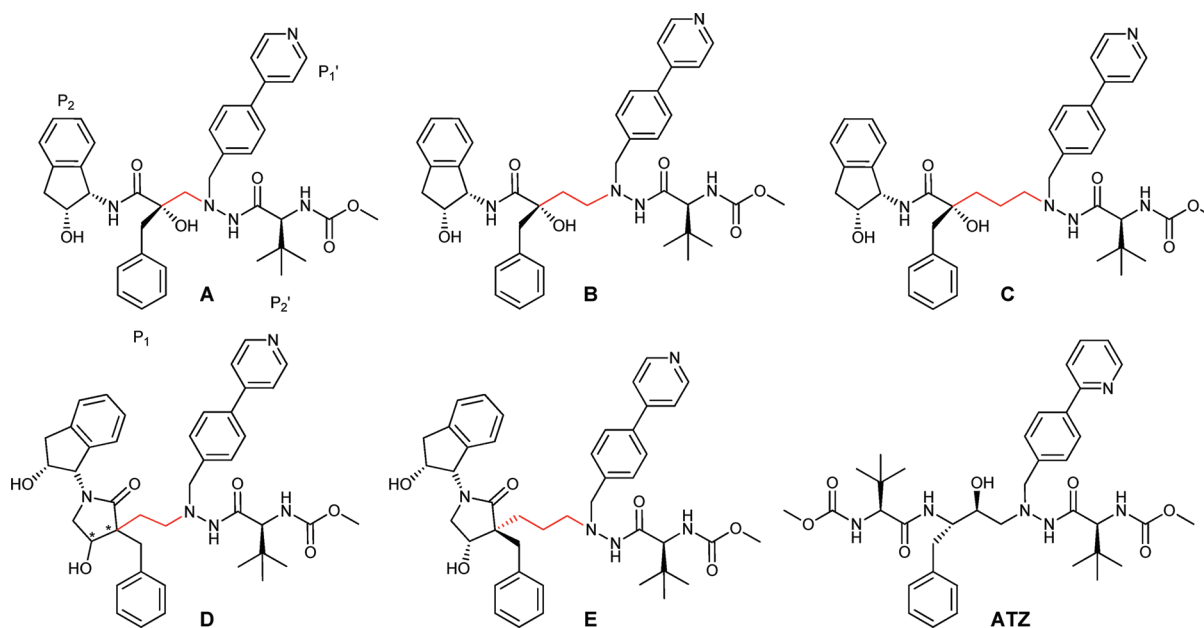
Figure 1. Examples of the previous series of tertiary alcohol-containing HIV-1 PIs. Spacers are indicated in red: **A**, one-carbon spacer (K_i = 5.5 nM);[23−25] **B**, two-carbon spacer (K_i = 2.3 nM);[26] **C**, three-carbon spacer (K_i = 2.8 nM);[27] **D**, novel lactam-based inhibitors with two-carbon spacer (K_i = 0.8 nM) and altered stereocenters indicated by asterisks; **E**, three-carbon spacer (K_i = 4.2 nM). ATZ is included for comparison (K_i = 2.7 nM).[37]

and 3 nM, respectively.[26] In all three series (**A**−**C**), inhibitors with high membrane permeability were identified, as well as inhibitors with good metabolic stability,[23−28] providing pharmacokinetic properties well in the range of HIV PIs already on the market, e.g., ATZ.[23]

X-ray analyses of inhibitors in series **A**−**C** cocrystallized with the enzyme revealed binding modes that were not completely successful in establishing strong symmetric hydrogen bonds (<3.0 Å) with both the catalytic residues Asp25 and or Asp125, originating from each monomer of the HIV-1 protease.[32−34] Therefore, we decided to further elaborate the central transition-state mimic by relocating the hydroxyl group one position away from the backbone. This strategy was implemented by making use of a β-hydroxy γ-lactam moiety equipped with a secondary alcohol. It was hypothesized that the β-hydroxy γ-lactam would provide a better hydrogen bond arrangement for the catalytic Asp residues and at the same time reduce the flexibility, providing a more rigid inhibitor.[35,36]

Modeling studies supported the hypothesis that a hydroxyl group in the 4-position of the γ-lactam might provide a new conformationally constrained transition-state-mimicking scaffold for the development of novel HIV-1 PIs. Since both the (3*R*,4*S*) and the (3*R*,4*R*) stereoisomers provided good docking poses, we decided to synthesize and evaluate all four stereoisomers of the γ-lactam (Figure 1, **D**). In addition, two different lengths of the central tether (two or three carbons) were investigated (Figure 1, **D** and **E**). The prime-side[31] hydrazide moiety, inspired by ATZ, has been successfully used in inhibitors in series **A**−**C** and was therefore retained in the new series of lactam-based inhibitors.

Here we present the synthetic protocols and the inhibitory potency on enzyme level, as well as the activity in a cell-based assay, of the new inhibitors (**D** and **E**). Also included are stability and permeability studies of selected compounds, together with X-ray analyses of three of the inhibitors cocrystallized with the HIV-1 protease.

■ CHEMISTRY

Starting from (*S*)-4-hydroxydihydrofuran-2(3*H*)-one (**1a**) or (*R*)-4-hydroxydihydrofuran-2(3*H*)-one (**1b**), four HIV-1 PR inhibitors with a two-carbon spacer and with varied stereochemistry in the lactam ring were synthesized (Scheme 1). Encouraged by previously reported alkylations,[38−40] **1a** and **1b** were chosen as starting substrates for the two-step alkylation process. Upon treatment with DMPU, LDA, and the first

Scheme 1. Dialkylation of Lactones 1a and 1b[a]
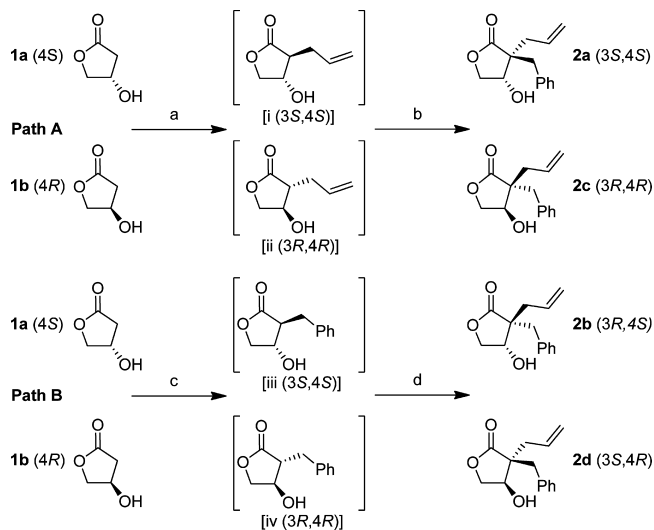
[a]Reagents and conditions. Path A: (a) DMPU, LDA, allyl bromide, dry THF, added at −50 °C, stirred at −50 °C for 1 h; (b) LDA, benzyl bromide added at −40 °C, stirred at −30 °C for 1 h, giving **2a** and **2c** in 49% and 33% isolated yield, respectively. Path B: (c) DMPU, LDA, benzyl bromide, dry THF, added at −50 °C, stirred at −40 °C for 1 h; (d) LDA, allyl bromide, added at −40 °C, stirred at −30 °C for 1 h, giving **2b** and **2d** in 2% and 5% isolated yield, respectively.

Scheme 2. Diastereomeric Enrichment of 2b and 2d[a]
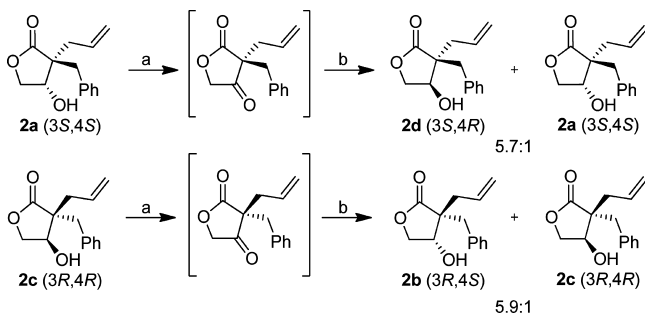
[a]Reagents and conditions: (a) **2a** or **2c**, Dess–Martin, DCM, rt, 1 h; (b) NaBH$_4$, 1% methanol in THF, rt 2 h, **2d** + **2a** (5.9:1) 92%, **2b** + **2c** (5.7:1) 85%.

Scheme 3. Lactamization of Lactones 2a–d[a]
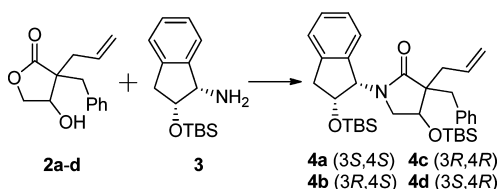
[a]Reagents and conditions: (i) [bmim]BF$_4$, 180 °C, 35 min; (ii) triethylamine, TBSOTf, DCM, 0–25 °C, overnight, giving isolated yields of **4a** 64%, **4b** 53%, **4c** 72%, and **4d** 50%.

alkylating agent (allyl bromide or benzyl bromide) at −50 °C followed by a second portion of LDA and the addition of the second alkylating agent (benzyl bromide or allyl bromide) at −40 °C, the dialkylated β-hydroxy γ-lactams **2a–d** were synthesized in isolated yields of 2−49% (Scheme 1, paths A and B).

In the first alkylation, the allyl group in **2a** and **2c** (or the benzyl group in **2b** and **2d**) was introduced trans to the controlling 4-hydroxyl group as expected, showing facial selectivity, as previously reported by Meyers et al.[41] and others.[39,40,42] In the second alkylation, the benzyl group (or the allyl group in **2b** and **2d**) was introduced trans to the 4-hydroxyl functionality. Consequently, the second alkylation changed the stereochemistry of the first inserted group, forcing it to end up cis to the 4-hydroxyl group.[40]
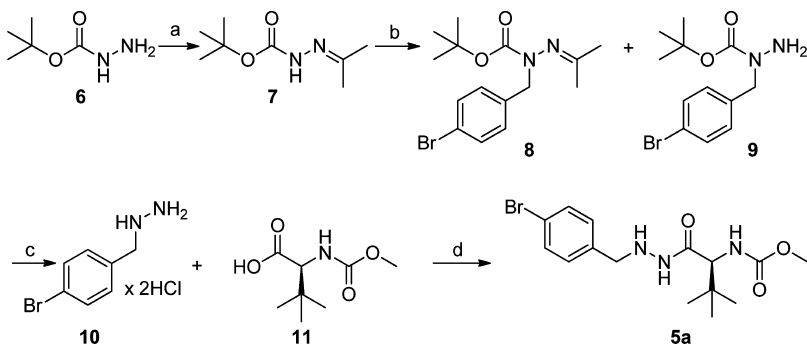
To be able to collect enough material of **2b** and **2d**, with their low-yielding synthetic pathway, a method was developed to alter the stereochemistry at the hydroxyl group in **2a** and **2c**. Oxidation of **2a** and **2c** with Dess−Martin reagent to the corresponding ketones was followed by reduction using NaBH$_4$, affording **2d** and **2b** following paths A and B, respectively (Scheme 2), with ratios **2d/2a** of 5.7:1 and **2b/2c** of 5.9:1. The diastereomers were separated on a silica flash column.

Lactamization of the lactones **2a−d** with TBS-protected indanolamine (**3**) was performed by adopting the methodology developed by Orrling et al.[43] (Scheme 3). Lactams **4a−d** were isolated in good yields using the ionic liquid 1-butyl-3-methylimidazolium tetrafluoroborate ([bmim]BF$_4$)[44] under microwave irradiation at 180 °C for 35 min, followed by protection of the alcohol moiety with TBSOTf under basic conditions.[45,46] (Scheme 3). Although the mixture was heated to 180 °C, these lactamization conditions are relatively mild compared to those previously reported.[47] The use of highly polar [bmim]BF$_4$ allowed lactamization to proceed smoothly without the need of Brønstedt acid.[43]

To synthesize the prime-side moiety **5a**, hydrazone **7** was prepared in almost quantitative yield starting from the BOC-protected hydrazine **6**, as previously reported in the literature[48] (Scheme 4). Benzylation of **7** using KOH and 4-bromobenzyl bromide in anhydrous toluene afforded **8** in good yield. Catalytic quantities of the phase-transfer catalyst tetrabutylammonium hydrogen sulfate (TBAHS) were used to improve solubility and increase the rate of the reaction.[49,50]

After the initial workup of the alkylation reaction only compound **8** was generated, but after flash chromatography purification, compound **9** was also formed (owing to hydrolysis of the hydrazone). However, purification in this step was necessary to remove excess quantities of 4-bromobenzyl bromide, which was foreseen to cause problems in the later steps. The mixture of **8** and **9** was deprotected with 4 M HCl in THF to yield the pure hydrochloride salt of **10**.

Owing to the photosensitivity of the free nitrogen in the p-bromobenzylhydrazine **10**, the coupling of **10** with **11**, synthesized as previously reported,[23] was performed in a reaction vessel wrapped in aluminum foil. Moreover, **10**, **11**, and HOBt were added under a nitrogen atmosphere at 0 °C, and the mixture was stirred for 30 min. Subsequently, 4-methylmorpholine (NMM) and N-(3-dimethylaminopropyl)-N′-ethylcarbodiimide hydrochloride (EDC) were added and the

Scheme 4. Synthesis of the Prime Side (5a)[a]

[a]Reaction conditions: (a) acetone, MgSO$_4$, AcOH (cat.), reflux, 1 h, 98%; (b) (i) KOH, anhydrous toluene, TBAHS, 50 °C, 20 min; (ii) **3**, 100 °C, 2 h, 81%; (c) HCl, THF, reflux, 3 h, quantitative yield; (d) EDCI, HOBt, NMM, DCM, 0−25 °C, 15 h, 77% (61% isolated yield over four steps.). Steps a and c required no purification.

Scheme 5. Oxidation and Reductive Amination To Give Two-Carbon-Spacer-Containing HIV-1 PIs 13a−d[a]

4a (3S,4S)
4b (3R,4S)
4c (3R,4R)
4d (3S,4R)

[v (3R,4S)]
[vi (3S,4S)]
[vii (3S,4R)]
[viii (3R,4R)]

12a (3R,4S)
12d (3R,4R)

13a (3R,4S)
13b (3S,4S)
13c (3S,4R)
13d (3R,4R)
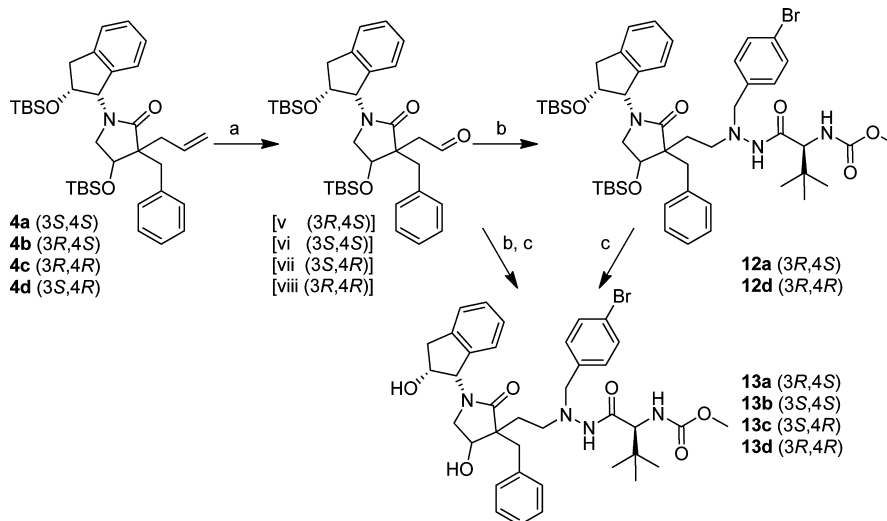
[a]Reagents and conditions: (a) 4a−d, OsO$_4$, NaIO$_4$, THF/H$_2$O, rt, overnight; (b) 5a, acetic acid, Na(OAc)$_3$BH, dry THF, rt, overnight, provided 12a in 35% and 12d in 54% isolated yield from 4a and 4d, respectively; (c) TBAF, THF, rt, overnight, provided 13a in 38%, 13b in 60%, 13c in 46%, 13d in 34% isolated yield from 4a−d, respectively.

Scheme 6. Synthesis of the 2-Pyridyl-Substituted Two-Carbon-Spacer-Containing HIV-1 PIs 13e−f[a]

14a (3R,4S)
14d (3R,4R)

[v (3R,4S)]
[viii (3R,4R)]

5b

15a (3R,4S)
15d (3R,4R)

13e (3R,4S)
13f (3R,4R)
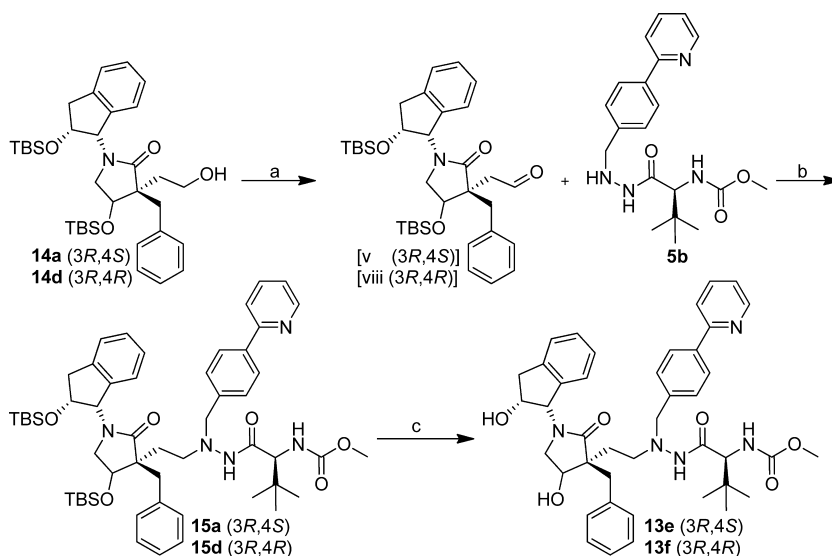
[a]Reagents and conditions: (a) 14a or 14d, Dess−Martin reagent, dry DCM, rt, 1 h; (b) acetic acid, Na(OAc)$_3$BH, dry THF, rt, overnight; (c) TBAF, THF, rt, overnight, provided isolated yields of 63% 13e and 38% 13h from 14a and 14d, respectively.

Scheme 7. Suzuki−Miyaura Decoration of 12a and 12d To Provide the Two-Carbon-Spacer-Containing HIV-1 PIs 13g−j[a]

12a (3R,4S)
12d (3R,4R)

13g (3R,4S) 13i (3R,4S)
13h (3R,4R) 13j (3R,4R)
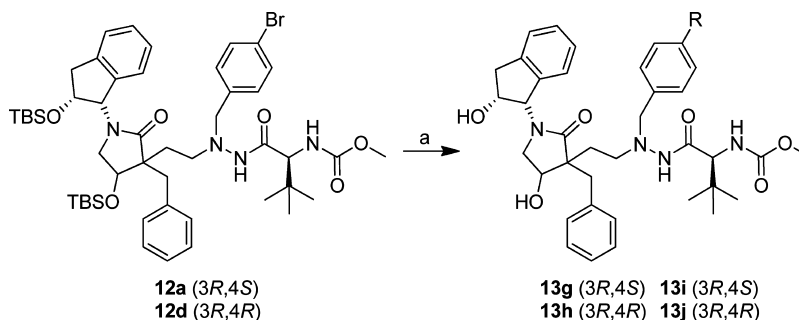
[a]Reagents and conditions: (a) (i) 12a or 12d, Herrmann's palladacycle, K$_2$CO$_3$, 3- or 4-pyridylboronic acid, [HP(t-Bu)$_3$]BF$_4$, DME, water, microwave 140 °C, 20 min; (ii) TBAF, THF, rt, overnight, providing isolated yields of 63% 13g, 59% 13h, 74% 13i, and 66% 13j.

Scheme 8. Synthesis of Three-Carbon-Spacer-Containing HIV-1 PIs 19a–e[a]
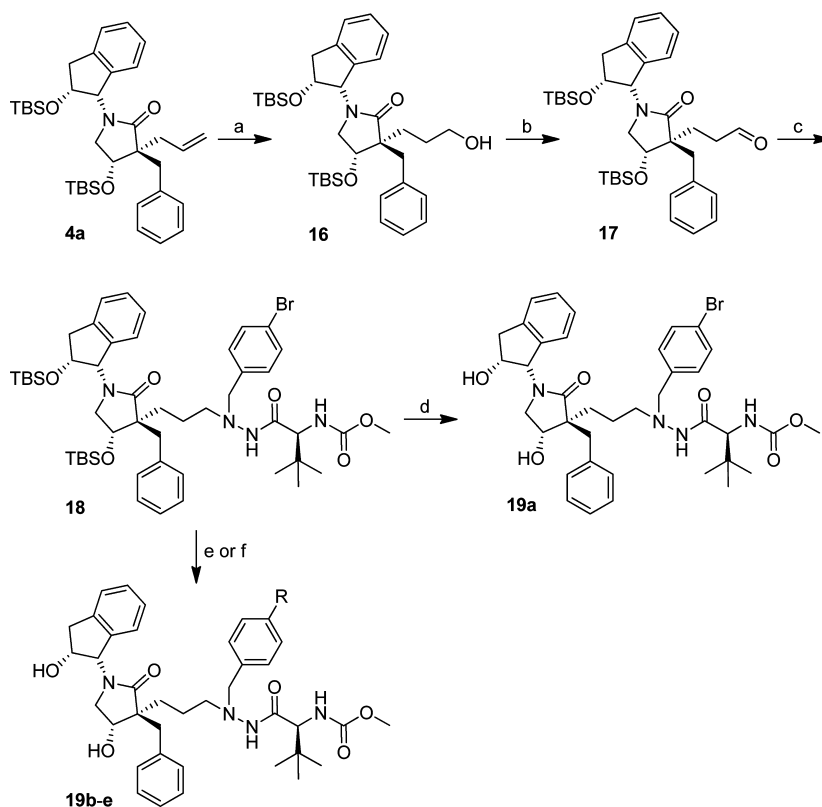
[a]Reagents and conditions: (a) (i) 9-BBN, dry THF, 80 °C, 6 h; (ii) 2 M NaOH, 30% H_2O_2 in H_2O, ethanol, rt, 2 h, 78%; (b) Et$_3$N, 50% SO$_3$Py in DMSO, dry DCM, 0–20 °C, 3 h; (c) **5a**, acetic acid, Na(OAc)$_3$BH, dry THF, 35 °C, 3 h, 35%; (d) TBAF, THF, rt, overnight, **19a** 61%; (e) (i) Herrmann's palladacycle, K$_2$CO$_3$, arylboronic acid, [HP(t-Bu)$_3$]BF$_4$, 105 °C, 1.5 h; (ii) TBAF, THF, rt, overnight, **19b** 45%, **19c** 35%, and **19d** 30%; (f) (i) 2-(tributylstannyl)pyridine, Pd(PPh$_3$)$_2$Cl$_2$, CuO, DMF, 105 °C, 2 h; (ii) TBAF, THF, rt, overnight, **19e** 16%.

---

reaction mixture was gradually heated to 25 °C and stirred under a nitrogen atmosphere for 15 h, giving **5a** in good isolated yield (77%, 61% overall isolated yield starting from 38 mmol of **6**).

Next the allylic double bonds in lactams **4a–d** were oxidatively cleaved to give the corresponding aldehydes **v–viii** using osmium tetraoxide and sodium periodate in THF/water (3:1) at room temperature[36,51] (Scheme 5). Note that the nomenclature for the absolute configuration for the lactam carbon in position 3 changes when comparing the lactams **4a–d**, the intermediates **v–viii**, and **12** and **13** because of changes in the assigned priority according to the sequence rule.[52,53]

The aldehydes were quickly flushed through a short silica column. Reductive amination between the crude aldehydes and the prime side (**5a**) was performed in dry THF using acetic acid, followed by treatment with Na(OAc)$_3$BH, to afford the crude TBS-protected products. The TBS protecting groups were removed using TBAF, and the inhibitors **13a–d**, carrying a two-carbon tether, were isolated in good yields (Scheme 5). The TBS-protected inhibitors **12a** and **12d** (but not **12b** and **12c**) were isolated, purified, and fully characterized before the final deprotection.

To evaluate the effect of different P1′ side chains, a small series of P1′ *p*-phenyl- and *p*-pyridyl-substituted inhibitors was produced. The known problem of rapid protodeboronation of 2-pyridylboronic acid[54] prevented us from conducting functionalization of **12a** and **12d** directly via Suzuki–Miyaura cross-coupling. Thus, to introduce the 2-pyridyl as a para-substituent in P1′, the 2-pyridine-substituted hydrazide **5b**

(Scheme 6) was synthesized starting from the 4-(2-pyridinyl)-benzaldehyde, as previously described.[27]

The alcohols **14a** and **14d** were isolated as side products in reductive amination reactions to produce **12a** and **12d**, respectively. Dess–Martin reagent was used to oxidize **14a** and **14d** to the corresponding aldehyde intermediates (Scheme 5, **v** and **viii**, respectively), followed by reductive amination with **5b** using acetic acid and Na(OAc)$_3$BH in dry THF and subsequent TBAF-mediated deprotection to give useful yields of the inhibitors **13e** and **13f** (Scheme 6).

The TBS-protected inhibitors **12a** and **12d** were decorated using the corresponding phenyl- or pyridylboronic acids in Suzuki–Miyaura cross-coupling in which Herrmann's palladacycle (0.1 equiv) was used as a palladium precatalyst together with K$_2$CO$_3$ (3.3 equiv) and [HP(t-Bu)$_3$]BF$_4$ (0.2 equiv) in DME/water. The reaction mixtures were heated to 140 °C for 20 min under focused microwave irradiation in sealed reaction vessels.[55−57] Cross-coupling was followed by deprotection of the hydroxyl groups using TBAF in THF at room temperature, giving inhibitors **13g–j** in good isolated yields (Scheme 7 and Table 2).

To be able to incorporate the new lactam scaffold into inhibitors with the three-carbon spacer, corresponding to the previously published **C** series (Figure 1), the allylic compound **4a** was refluxed in THF at 80 °C with 9-BBN for 6 h. After addition of NaOH, H$_2$O$_2$, and ethanol at room temperature and another 2 h stirring, the primary alcohol **16** was isolated in good yield (Scheme 8).[58] The alcohol **16** was oxidized to the

Table 1. Isolated Yields, Enzyme Inhibition Data, and Antiviral Activity of 12a, 12d, and 13a–d[a]

Compound	Structure	Yield[b] (%)	$K_i{}^{c}$ (nM)	EC$_{50}$ (µM)	CC$_{50}$ (µM)	CL$_{int}{}^{e}$ (µL/min/mg)	P$_{app}{}^{f}$ (× 10^{-6} cm/s)
12a		35	760	>10	>50	*	*
12d		54	800	>10	>50	*	*
13a		38	2.1	0.64	>50	>300	*
13b		62	1200	>10	15	*	*
13c		46	940	>10	>50	*	*
13d		34	6.4	0.35	>50	>300	17

[a]For preparation of inhibitors, see Scheme 5. The asterisk (∗) indicates not determined. [b]Isolated yields in the final reductive amination (12a, 12d) or reductive amination−deprotection step (13a–d). [c]ATZ: K_i = 2.7 nM.[37] [d]ATZ: EC$_{50}$ = 0.0039 mM.[37] [e]ATZ Cl$_{int}$ = 90 µL min^{-1} mg^{-123} [140 µL min^{-1} mg^{-164}]. [f]ATZ P$_{app}$(Caco-2) = 5.3 × 10^{-6} cm/s.

corresponding aldehyde (17) using 50% SO$_3$Py in DMSO together with triethylamine in DCM at 0−25 °C.[59,60]

The aldehyde was thereafter used in a reductive amination reaction with 5a using Na(OAc)$_3$BH as reducing agent at 35 °C to give 18 in moderate isolated yield (Scheme 8). The nomenclature for the absolute configuration of the lactam carbon in position 4 changes when comparing the 13a−j and 19a−e series because of changes in the assigned priority according to the sequence rule in IUPAC's guidelines.[52,53]

Deprotection of 18 using TBAF in THF gave inhibitor 19a in a good yield. Inhibitor 18 was also used as starting material in Suzuki−Miyaura cross-coupling with phenyl- and pyridylboronic acids together with Herrmann's palladacycle, K$_2$CO$_3$, and [HP(tBu$_3$)]BF$_4$, heated by microwave irradiation to 105 °C for 1.5 h. Deprotection of the TBS groups using TBAF in THF gave 19b−d in 35−40% isolated yields. By use of 2-(tributylstannyl)pyridine, compound 18 was subjected to Stille type coupling in DMF under microwave irradiation (105 °C, 2 h) using CuO and with Pd(PPh$_3$)$_2$Cl$_2$ as precatalyst.[61−63] The Stille coupling was followed by TBAF-mediated deprotection giving inhibitor 19e in moderate isolated yield.

■ RESULTS

Since the preliminary docking studies suggested that two of the stereoisomers in the lactam moiety ((3R,4S) and (3R,4R)), in the two-carbon-tethered inhibitors would fit well in the enzyme, all four stereoisomers were synthesized and evaluated regarding binding and in a cell-based assay, giving the results summarized in Table 1. Comparisons with previous series of tertiary-alcohol-based HIV-1 PIs (A−C) could easily be conducted by using the indanolamide in the P2 position and the p-bromophenyl as the P1′ side chain.

In accordance with the initial docking studies, inhibitors 13a (3R,4S) and 13d (3R,4R) exhibited good activity in the enzyme assay (K_i of 2.1 and 6.4 nM, respectively) as well as in the cell-based evaluation (EC$_{50}$ of 0.64 and 0.35 µM, respectively). The stereoisomers 13b (3S,4S) and 13c (3S,4R) did not show any activity and, as expected, neither did the TBS-protected inhibitors 12a and 12d. The metabolic stability and permeability of the two active inhibitors were investigated. High metabolic clearance was observed for both 13a and 13d. However, 13d also showed good results in the Caco-2 permeability study. Because of its low solubility, inhibitor 13a was not tested in the permeability assay. Compound 13b exhibited slight cell toxic properties, with a CC$_{50}$ of 15 µM.

The lactam scaffold inhibitors 13a and 13d ((3R,4S) and (3R,4R), respectively) yielded the most potent inhibitors and were therefore selected for further optimization.

When the P1′ position is optimized by replacing the p-bromo substituent of the P1′ phenyl group in 13a and 13d with heteroaromatic moieties, the inhibitors showed improved protease inhibitor potency and, most importantly, increased antiviral activity (Table 2, 13e−j).

Table 2. Isolated Yields, Enzyme Inhibition Data, and Antiviral Activity of Compounds 13g−j[a]

Compound	Structure	Yield[b] (%)	K_i[c] (nM)	EC$_{50}$ (μM)	CC$_{50}$ (μM)	CL$_{int}$[e] (μL/min/mg)	P$_{app}$[f] (× 10^{-6} cm/s)
13e		48	1.7	0.19	28	*	*
13f		38	2.0	0.18	>50	*	*
13g		63	0.8	0.040	>50	230	3.8
13h		59	0.7	0.10	>50	120	5.1
13i		74	0.4	0.040	>50	*	*
13j		66	1.7	0.096	>50	*	*
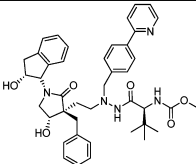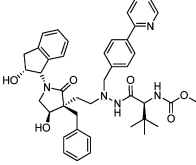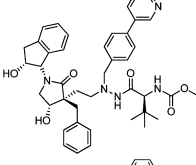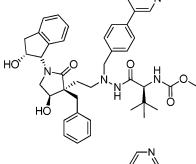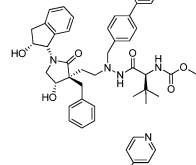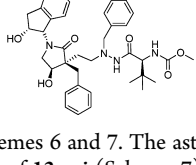
[a]For preparation of inhibitors, see Schemes 6 and 7. The asterisk (∗) indicates not determined. [b]Isolated yields of 13e−f from 14a or 14d (Scheme 6) or in the coupling deprotection step of 13g−j (Scheme 7). [c]ATZ: K_i = 2.7 nM.[37] [d]ATZ: EC$_{50}$ = 0.0039 mM.[37] [e]ATZ Cl$_{int}$ = 90 μL min^{-1} mg^{-1} [23] [140 μL min^{-1} mg^{-1} [64]]. [f]ATZ P$_{app}$(Caco-2) = 5.3 × 10^{-6} cm/s.

The best inhibitors, having (3R,4S) configuration and 3- or 4-pyridylbenzyl as the P1′ moiety (13g and 13i), exhibited 10 times higher potency than 13a in the cell-based antiviral activity assay, the best EC$_{50}$ values being 40 nM (Table 2). The 2-pyridyl-substituted inhibitor (13e) showed lower activity than the 3- and 4-pyridyl-substituted analogues (13g and 13j, respectively). The improved EC$_{50}$ upon decorations with 2-, 3-, and 4-pyridyls has previously been demonstrated showing the same trend.[24]

The (3R,4R) compounds showed less improvements, but all inhibitors decorated with pyridine functionalized in P1′ were observed to have higher potency than the precursor bromo compound 13d. The position of the nitrogen in the heteroaromatic P1′ group showed the same general trend as in the (3R,4S) inhibitors, with the meta- and para-positions providing the best potency (Table 2).

Heteroaromatic functionalization of P1′ provided inhibitors with increased stability compared to 13a and 13d. Compound 13h gave the best result (Cl$_{int}$ of 120 μL min^{-1} mg^{-1}). Both 13g and 13h were observed to possess moderate permeability in the Caco-2 studies, with P$_{app}$ of 3.8 × 10^{-6} and 5.1 × 10^{-6} cm/s, respectively.

When the backbone spacer was elongated from two to three carbons, as in 19a−e, inhibitors with lower potency than the 13 series were obtained (Table 3). This is in accordance with results previously reported for the linear series of tertiary alcohol inhibitors, e.g., comparing the B[26] and C[27] series (Figure 1). However, with the p-phenyl or p-4-pyridyl groups in the P1′ position, submicromolar values of EC$_{50}$ were observed in the antiviral cell based assay (19b and 19d).

As mentioned above, permeability (Caco-2) and stability (Cl$_{int}$) studies were performed on some of the inhibitors prepared (13a, 13d, 13g, 13h, 19a, 19c, and 19e). Compound 19a showed high permeability (>20 × 10^{-6} cm/s), while all other inhibitors investigated showed moderate permeability ((3−20) × 10^{-6} cm/s). The value of Cl$_{int}$ varied from 120 to >300 μL min^{-1} mg^{-1} (Tables 1−3). These results are in the same range as those previously reported for ATZ (P$_{app}$ = 5.3 × 10^{-6} cm/s, Cl$_{int}$ = 90 μL min^{-1} mg^{-1} [23] [140 μL min^{-1} mg^{-1} [64]]). There was no major difference between the 13 and the 19 series with respect to Cl$_{int}$ and P$_{app}$, and the rigidification of the backbone seemed to be well tolerated compared to the linear inhibitors.[23,27,28] The metabolic stability was improved when the bromo group in 13a and 19a was

Table 3. Isolated Yields, Enzyme Inhibition Data, and Antiviral Activity for Compounds 19a–e[a]

Compound	Structure	Yield[b] (%)	K_i[c] (nM)	EC_{50} (μM)	CC_{50} (μM)	CL_{int}[e] (μL/min/mg)	P_{app}[f] (× 10^{-6} cm/s)
19a		61	13	3.9	26	>300	22
19b		45	12	0.85	15	*	*
19c		35	5.3	1.8	23	122	4.4
19d		30	4.2	0.7	5.9	*	*
19e		16	6.3	2.5	31	130	3.4

[a]For conditions, see Scheme 8. The asterisk (*) indicates not determined. [b]Isolated yields of **19a** for the deprotection step, and isolated yields of **19b–e** for the coupling–deprotection step. [c]ATZ: K_i = 2.7 nM.[37] [d]ATZ: EC_{50} = 0.0039 mM.[37] [e]ATZ CL_{int} = 90 μL min^{-1} mg^{-1}[23] [140 μL min^{-1} mg^{-1} [64]]. [f]ATZ P_{app}(Caco-2) = 5.3 × 10^{-6} cm/s.

substituted by the heteroaromatic pyridyls, although the permeability was unfortunately reduced at the same time.

X-ray Structure Analysis. A drug-resistant strain of the HIV-1 protease (Leu63Pro, Val82Thr, Ile84Val)[65] was cocrystallized with the active PIs **13i**, **19b**, and **19d** for X-ray crystallographic studies of the complexes. Data were obtained for all complexes, and the structures were refined to high resolution (for refinement statistics, see Supporting Information). The resulting electron density maps allowed unambiguous modeling of the inhibitors within the binding site. Overviews of the binding patterns are presented in Figure 2. Previously published structures of HIV-1 PIs **20**,[27] **21**,[28] and ATZ[29] are included for comparison (Figure 3).

A complicating factor for the comparisons of the inhibitor complexes was the fact that compounds **20** and ATZ were rotated 180° compared to compounds **13i**, **19b**, **19d**, and **21**.[66–68]

The amino acids are labeled according to the novel inhibitor–enzyme complexes presented herein (**13i**, **19b**, and **19d**). The overall binding configurations for **13i**, **19b**, and **19d** to the protease are, as expected, in good accordance with those of previously published linear inhibitors **20**,[27] **21**,[28] as well as with ATZ, despite the novel β-hydroxy γ-lactam moiety.

Lactam Moiety. On the basis of the modeling studies, it was postulated that the β-hydroxyl group of the lactam moieties forms hydrogen bonds with the catalytic aspartic acids (Asp25 and Asp125).

In the two-carbon linker compound **13i** this β-hydroxy group forms hydrogen bond interactions to the two catalytic aspartic acids with 2.7 and 3.0 Å. The β-hydroxy group in the three-carbon inhibitors **19b** and **19d** only form hydrogen bonds to Asp25, with 2.7 and 2.6 Å, respectively (Figure 2). This loss of a hydrogen bond for the **19** series compounds is due to the different spatial conformation of the lactam ring, apparently as a result of the longer central backbone (Figure 4). As the only difference between the structures of **13i** and **19d** is the length of the backbone tether, this is a likely explanation of the lower antiviral potency of compound **19d** compared with **13i**.

None of the cocrystallized PIs in these novel series formed a symmetrical binding pattern with the catalytic aspartic acids (Asp25 and Asp125) such as that seen in ATZ. Together with the hydrazide carbonyl oxygen, the carbonyl oxygen in the lactam ring in both **13i** and **19d** creates hydrogen bonds to the structural water bridging the inhibitors and the Ile50 and Ile150 in the flap region with hydrogen bond lengths of 2.7–3.3 Å (Figure 2).

The position of the P2–P3 indanolamide in **13i**, **19b**, and **19d** is not markedly affected by the introduction of the β-hydroxy γ-lactam, absent in **20**. While in **20** the indanolhydroxyl group was close enough to form a hydrogen bond to Arg108 and for the Arg108 to make an edge-on cation–π interaction with the P1 phenyl group, the distance to the indanol group in **13i** seems to prevent this bond from forming (Figure 5).
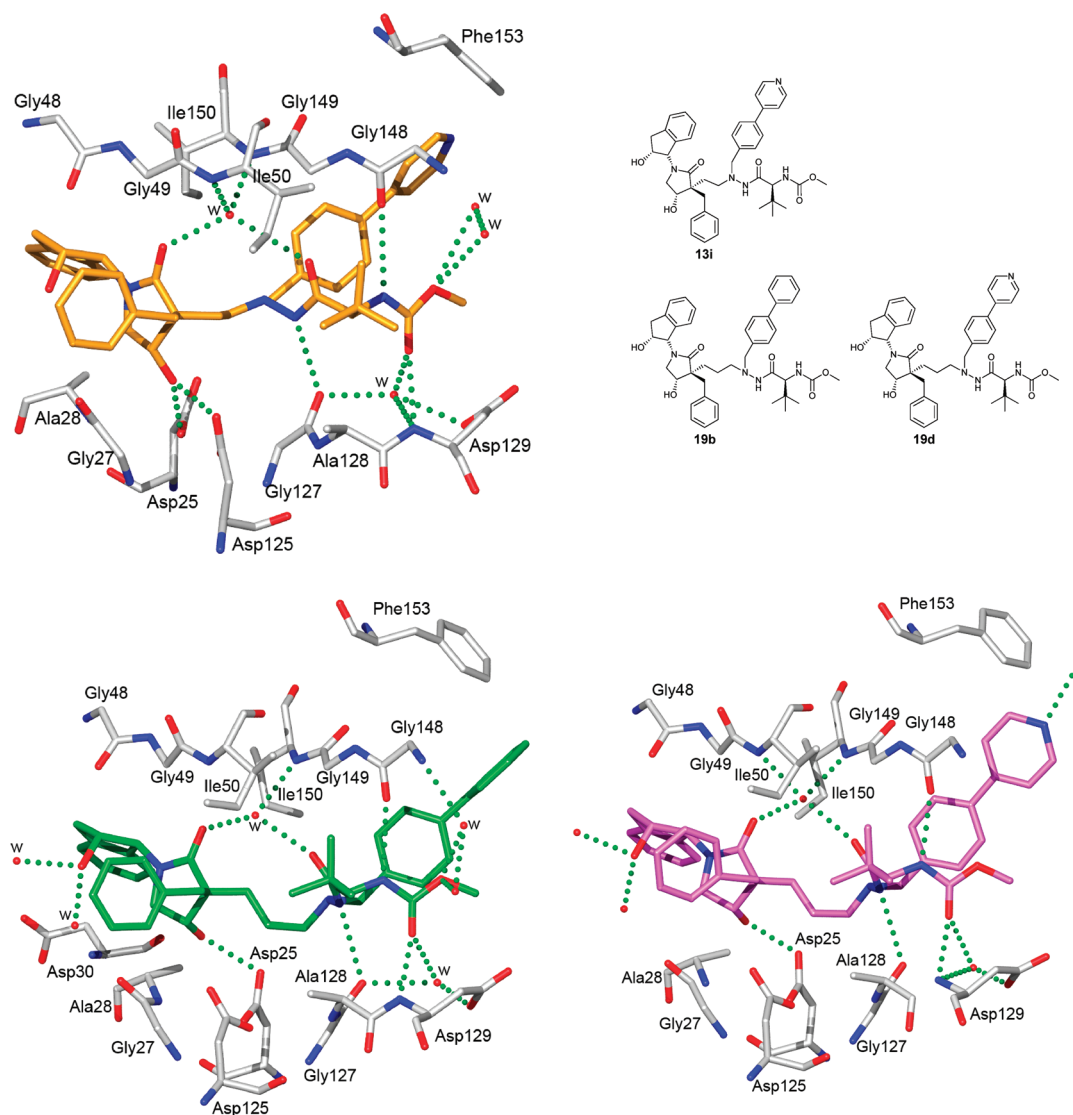
Figure 2. Comparison of the overall X-ray conformations and binding patterns of compounds **13i** (top left, PDB code 2uxz), **19b** (bottom left, PDB code 4a6c), and **19d** (bottom right, PDB code 4a6b) in the active site of HIV-1 protease. Compound **13i** forms five direct hydrogen bonds to the protease and five more via water molecules. The corresponding binding interactions for **19b** and **19d** are four direct bonds and six more through water bridges. In all three complexes, two of the interactions via water are due to the structural water coordinating Ile50 and Ile150 in the protein flaps.

P1′ Site. In accordance with the previously observed results for **21**,[28] the P1′ outer phenyl group in both **13i** and **19d** interacts through a hydrophobic interaction with Pro81 (3.3–3.8 Å) and an edge–face π–π interaction to Phe153 (3.7–3.8 Å). The differences in length of the central motif as well as in the length of the extension of **13i**, **19d**, **20**, **21**, and ATZ in the P1′ site are nicely accommodated through corresponding shifts in the positions of Phe153 and Pro81 (Figure 5).[28]

These interactions are likely to improve the binding constant and is the most likely explanation of the better binding of compound **13i** than **13d**, differing only in the length of the extension in the P1′ site. In a previously examined complex with compound **20**, the interaction with Phe153 was not possible, as the corresponding moiety only reached far enough for a van der Waal interaction with Pro81. Neither is the interaction with Phe153 observed in the complex with ATZ. Since the binding modes of **19b** and **19d** are very similar (Figure 2), only **19d** was included in the analysis, as the structure of the complex could be interpreted at higher resolution.

DISCUSSION

Chemistry. The introduction of the β-hydroxy γ-lactams as new scaffolds was intended to provide more rigid PIs and to relocate the hydroxyl group from the backbone to enable more symmetric binding to the catalytically active Asp25 and Asp125 of the HIV-1 protease. The outcome of the dialkylation reactions performed to obtain **2a–d** was in accordance with the results described by Amat et al. in 2007, although they observed a larger substrate-dependent variability.[69] When introducing the benzyl moiety in the first alkylation, as in the cases of **2b** and **2d**, the yields were lower (2% and 5%, respectively) than when the allyl group was introduced before the benzyl moiety (as in **2a** and **2c**, with yields of 49% and 33%, respectively). The same trend has been reported by Johnson et al. with 4-substituted lactams[40] but was not observed in the 5-substitued examples presented by Meyers et al., in which the order of addition did not affect the yields.[41] Probable reasons for the lower yields observed by Johnson et al. were steric and/or electrostatic
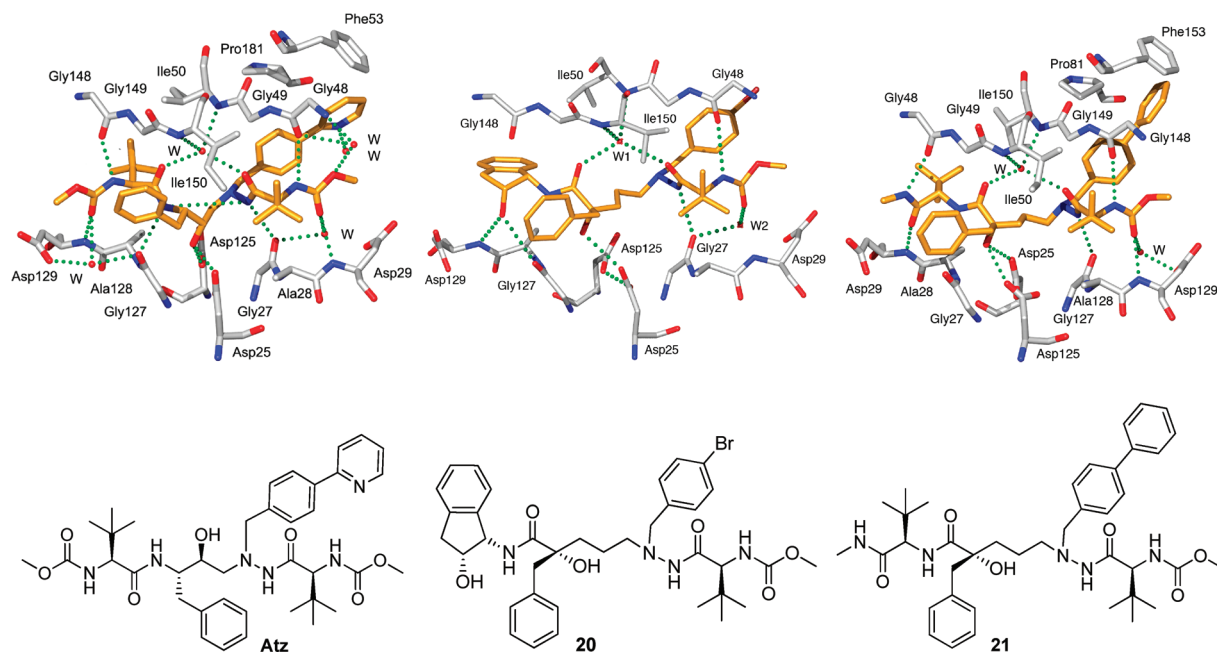
Figure 3. Previously published PIs for comparison: ATZ (PDB code 3EL9), **20** (PDB code 2uxz),[27] and **21** (PDB code 2xye).[28]

interactions between the 4-hydroxy group and the bulkier 3-benzyl moiety present after the first alkylation, compared to the smaller allyl group. These findings followed the reasoning presented by Huang et al.,[70] who proposed stereoelectronic

Figure 4. The position of the β-hydroxy group of the lactame ring, involved in hydrogen binding to both Asp25 and Asp125 in **13i** (gold), is different in **19d** (purple) and **19b** (not shown) exhibiting the three-carbon linker. This leads to a loss of a hydrogen bond to one of the catalytic aspartates. The position of the β-hydroxy group involved in hydrogen binding in **19d** is 2.1 Å from the position observed in **13i**.

factors to be the major explanation in this class of stereoselective two-step alkylation reactions.

In the present work, the diastereoselectivity controlled by the stereochemistry of the 4-hydroxy group was strong enough to allow highly enantiomerically enriched isomers to be obtained in all cases.

There was an urgent need for a robust method for the synthesis of the prime side hydrazide moiety (**5a**). The procedures used previously were cumbersome and low yielding because of the use of toxic and environmentally hazardous hydrazine hydrate and/or tedious purification protocols. Previously used synthetic procedures were not satisfactory, since the quantities of prime side were not sufficient to support our lead optimization program throughout. The synthetic route to the prime side hydrazide moiety **5a** presented here provided an efficient way of producing sufficient amounts and constitutes an improvement in yield as well as a reduction in work compared to previous methods.[27,71] With this convenient method, there was no need to use hazardous hydrazine hydrate, and the purification protocol resulted in a good yield.

Biological Evaluation and X-ray Structure Analysis. The biological results obtained from the novel lactam-containing inhibitors are summarized in Tables 1−3. Evaluation of the four stereoisomers (**13a−d**) gave two active and two nonactive PIs (Table 1). The (3R,4R) and (3R,4S) stereoisomers in the lactam ring showed the best results, with **13a** and **13d** being the most potent compounds (K_i < 10 nM and EC_{50} < 1 μM).

The most important structure−activity feature appears to be the direction of the benzyl in the P1 position. With R-stereochemistry at the α-carbon (**13a** and **13d**), the direction of the β-hydroxy substituent (position 4) appears to be of less importance for inhibition with **13a** and **13d** being almost equipotent. With S-stereochemistry at the α-carbon, **13b** and **13c** showed almost no inhibiting effect on the enzyme or in the cell-based antiviral activity assay (Table 1) and, as expected, the TBS-protected inhibitors **12a** and **12d** did not show any inhibitory potency.

Figure 5. Comparison of the positioning of the cocrystallized inhibitors in the S2−S3 pocket and interaction with Pro81 and Phe153 in the S1′ pocket. The effect on the S2−S3 site is visualized at residues Asp29, Asp30, Arg108, and Pro181. (a) Superimposition of **13i** (gold) and **19d** (purple). As a result of an additional CH_2 group in **19d**, the indanol group of **19d** dislocates Asp30 compared to **13i**. (b) Superimposition of **19d** and **20** (blue). The lactam group present in the new series of compounds as in **19d** mimics the conformation of **20**, also exhibiting the three-carbon linker, very well. With the lactam ring present, the position of the indanol ring, and therefore also Asp30/130, is more similar to the situation in **13i** comprising the two-carbon linker. (c) Superimposition of **13i** and ATZ (black). Despite the differences of functional elements between **13i** and ATZ in the S2−S3 site, the common ribbon of the compounds overlap well. In the P1′ site **13i** and **19d** extend further than ATZ, inducing spatial rearrangement of Phe153 and Pro81. Compound **19d** induced side chain and main chain atom displacements in Phe153 and Pro81 up to 2.5 and 1.7 Å, respectively, compared to ATZ complex positions. Corresponding displacements with **13i** as substrate are 0.9 and 0.5 Å. None of the new compounds induced a shift in the position of Arg108, as was seen in compound **20**.[27]

When the P1′ side chain was decorated with heteroaromatic moieties (Table 2), at best a 10-fold improvement in inhibitory potency was observed (**13g** and **13i**, EC$_{50}$ = 0.04 μM). Compared to the 2-pyridyl inhibitor **13e** (EC$_{50}$ = 0.190 μM), the 3- and 4-pyridyl-substituted inhibitors (**13g** and **13i**, respectively) with (3*R*,4*S*) stereochemistry afforded 5 times higher potency, with EC$_{50}$ of 40 nM. Despite the fact that ATZ contains a 2-pyridinyl in position P1′,[37] our previous series with one- or three-carbon spacers showed better potency for the 3- and 4-pyridinyl-substituted inhibitors.[24,27,28] With the linear two-carbon spacer the 2-, 3-, and 4-pyridinyls gave equipotent inhibitors.[26] This result was also obtained with the lactam-containing inhibitors with the three-carbon extended PIs in the **19** series.

Comparing *p*-bromide functionalized inhibitors **13a** and **19a**, a 5-fold loss of potency within measured K_i and EC$_{50}$ values were observed. However, the same trend is present in both series (**13** and **19**, Table 3) as seen with the shorter inhibitors. The pyridyls (**19c−e**) showed slightly better inhibition compared to the *p*-bromo compound **19a**. The *p*-phenyl substituted **19b** was among the most potent inhibitors, concurring with recent reports.[26,28]

CONCLUSIONS

We have successfully introduced β-hydroxy γ-lactams providing a rigid backbone moiety and replaced the previously used *tert*-hydroxy group with a *sec*-hydroxy group. All four stereoisomers were synthesized, incorporated into the full inhibitor and evaluated. In addition, the length of the central spacer was varied (two or three carbons). Functionalization of the two most potent stereoisomers (3*R*,4*S*) (**13a**) and (3*R*,4*R*) (**13d**) with heteroaromatic moieties in the *p*-benzyl P1′ position improved the potency, rendering K_i values down to 0.7 nM and EC$_{50}$ values down to 0.04 μM. Three inhibitors were cocrystallized with the HIV-1 protease enzyme providing information about the binding of the hydroxy lactams to the enzyme. The change in binding pattern between the inhibitors

with two- and three-carbon spacers was in good agreement with the observed variation in enzyme binding activity.

ASSOCIATED CONTENT

Ⓢ Supporting Information

Details of syntheses and reaction conditions, X-ray statistics, and description of biological assays. This material is available free of charge via the Internet at http://pubs.acs.org.

AUTHOR INFORMATION

Corresponding Author

*Phone: +46 18-471 4667. Fax: +46 18 471 4374. E-mail: mats.larhed@orgfarm.uu.se.

Notes

The authors declare no competing financial interest.

REFERENCES

(1) Barre-Sinoussi, F.; Chermann, J. C.; Rey, F.; Nugeyre, M. T.; Chamaret, S.; Gruest, J.; Dauguet, C.; Axler-Blin, C.; Vezinet-Brun, F.; Rouzioux, C.; Rozenbaum, W.; Montagnier, L. Isolation of a T-Lymphotropic Retrovirus from a Patient at Risk for Acquired Immune Deficiency Syndrome (AIDS). *Science* **1983**, *220*, 868−871.

(2) Gallo, R. C.; Sarin, P. S.; Gelmann, E. P.; Robert-Guroff, M.; Richardson, E.; Kalyanaraman, V. S.; Mann, D.; Sidhu, G. D.; Stahl, R. E.; Zolla-Pazner, S.; Leibowitch, J.; Popovic, M. Isolation of Human T-Cell Leukemia Virus in Acquired Immune Deficiency Syndrome (AIDS). *Science* **1983**, *220*, 865−867.

(3) *Global Report: UNAIDS Reoport on the Global AIDS Epidemic 2010*; UNAIDS: Geneva, 2010; 364 pp.

(4) Roberts, N. A.; Martin, J. A.; Kinchington, D.; Broadhurst, A. V.; Craig, J. C.; Duncan, I. B.; Galpin, S. A.; Handa, B. K.; Kay, J.; Krohn, A.; Lambert, R. W.; Merrett, J. H.; Mills, J. S.; Parkes, K. E. B.;

Redshaw, S.; Ritchie, A. J.; Taylor, D. L.; Thomas, G. J.; Machin, P. J. Rational Design of Peptide-Based HIV Proteinase-Inhibitors. *Science* **1990**, *248*, 358−361.

(5) Hammer, S. M.; Squires, K. E.; Hughes, M. D.; Grimes, J. M.; Demeter, L. M.; Currier, J. S.; Eron, J. J. Jr.; Feinberg, J. E.; Balfour, H. H. Jr.; Deyton, L. R.; Chodakewitz, J. A.; Fischl, M. A. A Controlled Trial of Two Nucleoside Analogues plus Indinavir in Persons with Human Immunodeficiency Virus Infection and CD4 Cell Counts of 200 per Cubic Millimeter or Less. AIDS Clinical Trials Group 320 Study Team. *N. Engl. J. Med.* **1997**, *337*, 725−733.

(6) Palella, F. J. Jr.; Delaney, K. M.; Moorman, A. C.; Loveless, M. O.; Fuhrer, J.; Satten, G. A.; Aschman, D. J.; Holmberg, S. D. Declining Morbidity and Mortality among Patients with Advanced Human Immunodeficiency Virus Infection. HIV Outpatient Study Investigators. *N. Engl. J. Med.* **1998**, *338*, 853−860.

(7) Mocroft, A.; Vella, S.; Benfield, T. L.; Chiesi, A.; Miller, V.; Gargalianos, P.; d'Arminio Monforte, A.; Yust, I.; Bruun, J. N.; Phillips, A. N.; Lundgren, J. D. Changing Patterns of Mortality across Europe in Patients Infected with HIV-1. *Lancet* **1998**, *352*, 1725−1730.

(8) Yeni, P. Update on HAART in HIV. *J. Hepatol.* **2006**, *44*, S100−S103.

(9) Pokorna, J.; Machala, L.; Rezacova, P.; Konvalinka, J. Current and Novel Inhibitors of HIV Protease. *Viruses* **2009**, *1*, 1209−1239.

(10) Ghosh, R. K.; Ghosh, S. M.; Chawla, S. Recent Advances in Antiretroviral Drugs. *Expert Opin. Pharmacol.* **2011**, *12*, 31−46.

(11) Carr, A. Toxicity of Antiretroviral Therapy and Implications for Drug Development. *Nat. Rev. Drug Discovery* **2003**, *2*, 624−634.

(12) Hawkins, T. Understanding and Managing the Adverse Effects of Antiretroviral Therapy. *Antiviral Res.* **2010**, *85*, 201−209.

(13) Walmsley, S. Protease Inhibitor-Based Regimens for HIV Therapy: Safety and Efficacy. *JAIDS, J. Acquired Immune Defic. Syndr.* **2007**, *45*, S5−S13.

(14) Mehellou, Y.; De Clercq, E. Twenty-Six Years of Anti-HIV Drug Discovery: Where Do We Stand and Where Do We Go? *J. Med. Chem.* **2010**, *53*, 521−538.

(15) Wensing, A. M. J.; van Maarseveen, N. M.; Nijhuis, M. Fifteen Years of HIV Protease Inhibitors: Raising the Barrier to Resistance. *Antiviral Res.* **2010**, *85*, 59−74.

(16) Randolph, J. T.; DeGoey, D. A. Peptidomimetic Inhibitors of HIV Protease. *Curr. Top. Med. Chem.* **2004**, *4*, 1079−1095.

(17) Anderson, J.; Schiffer, C.; Lee, S.-K.; Swanstrom, R. Viral Protease Inhibitors. *Handb. Exp. Pharmacol.* **2009**, *189*, 85−110.

(18) Este, J. A.; Cihlar, T. Current Status and Challenges of Antiretroviral Research and Therapy. *Antiviral Res.* **2010**, *85*, 25−33.

(19) Roberts, J. D.; Bebenek, K.; Kunkel, T. A. The Accuracy of Reverse-Transcriptase from HIV-1. *Science* **1988**, *242*, 1171−1173.

(20) Mastrolorenzo, A.; Rusconi, S.; Scozzafava, A.; Barbaro, G.; Supuran, C. T. Inhibitors of HIV-1 Protease: Current State of the Art 10 Years after Their Introduction. From Antiretroviral Drugs to Antifungal, Antibacterial and Antitumor Agents Based on Aspartic Protease Inhibitors. *Curr. Med. Chem.* **2007**, *14*, 2734−2748.

(21) Clavel, F.; Hance, A. J. HIV drug resistance. *N. Engl. J. Med.* **2004**, *350*, 1023−1035.

(22) Hulten, J.; Bonham, N. M.; Nillroth, U.; Hansson, T.; Zuccarello, G.; Bouzide, A.; Aqvist, J.; Classon, B.; Danielson, U. H.; Karlen, A.; Kvarnstrom, I.; Samuelsson, B.; Hallberg, A. Cyclic HIV-1 Protease Inhibitors Derived from Mannitol: Synthesis, Inhibitory Potencies, and Computational Predictions of Binding Affinities. *J. Med. Chem.* **1997**, *40*, 885−897.

(23) Ekegren, J. K.; Unge, T.; Safa, M. Z.; Wallberg, H.; Samuelsson, B.; Hallberg, A. A New Class of HIV-1 Protease Inhibitors Containing a Tertiary Alcohol in the Transition-State Mimicking Scaffold. *J. Med. Chem.* **2005**, *48*, 8098−8102.

(24) Ekegren, J. K.; Ginman, N.; Johansson, A.; Wallberg, H.; Larhed, M.; Samuelsson, B.; Unge, T.; Hallberg, A. Microwave-Accelerated Synthesis of P1′-Extended HIV-1 Protease Inhibitors Encompassing a Tertiary Alcohol in the Transition-State Mimicking Scaffold. *J. Med. Chem.* **2006**, *49*, 1828−1832.

(25) Ekegren, J. K.; Gising, J.; Wallberg, H.; Larhed, M.; Samuelsson, B.; Hallberg, A. Variations of the P2 Group in HIV-1 Protease Inhibitors Containing a Tertiary Alcohol in the Transition-State Mimicking Scaffold. *Org. Biomol. Chem.* **2006**, *4*, 3040−3043.

(26) Mahalingam, A. K.; Axelsson, L.; Ekegren, J. K.; Wannberg, J.; Kihlstrom, J.; Unge, T.; Wallberg, H.; Samuelsson, B.; Larhed, M.; Hallberg, A. HIV-1 Protease Inhibitors with a Transition-State Mimic Comprising a Tertiary Alcohol: Improved Antiviral Activity in Cells. *J. Med. Chem.* **2010**, *53*, 607−615.

(27) Wu, X.; Öhrngren, P.; Ekegren, J. K.; Unge, J.; Unge, T.; Wallberg, H.; Samuelsson, B.; Hallberg, A.; Larhed, M. Two-Carbon-Elongated HIV-1 Protease Inhibitors with a Tertiary-Alcohol-Containing Transition-State Mimic. *J. Med. Chem.* **2008**, *51*, 1053−1057.

(28) Öhrngren, P.; Wu, X.; Persson, M.; Ekegren, J. K.; Wallberg, H.; Vrang, L.; Rosenquist, A.; Samuelsson, B.; Unge, T.; Larhed, M. HIV-1 Protease Inhibitors with a Tertiary Alcohol Containing Transition-State Mimic and Various P2 and P1′ Substituents. *MedChemComm* **2011**, *2*, 701−709.

(29) Bold, G.; Fässler, A.; Capraro, H.-G.; Cozens, R.; Klimkait, T.; Lazdins, J.; Mestan, J.; Poncioni, B.; Rösel, J.; Stover, D.; Tintelnot-Blomley, M.; Acemoglu, F.; Beck, W.; Boss, E.; Eschbach, M.; Hurlimann, T.; Masso, E.; Roussel, S.; Ucci-Stoll, K.; Wyss, D.; Lang, M. New Aza-Dipeptide Analogues as Potent and Orally Absorbed HIV-1 Protease Inhibitors: Candidates for Clinical Development. *J. Med. Chem.* **1998**, *41*, 3387−3401.

(30) Piliero, P. J. Atazanavir: A Novel HIV-1 Protease Inhibitor. *Expert Opin. Invest. Drugs* **2002**, *11*, 1295−1301.

(31) Schechter, I.; Berger, A. On the Size of the Active Site in Proteases. I. Papain. *Biochem. Biophys. Res. Commun.* **1967**, *27*, 157−162.

(32) Miller, M.; Schneider, J.; Sathyanarayana, B. K.; Toth, M. V.; Marshall, G. R.; Clawson, L.; Selk, L.; Kent, S. B. H.; Wlodawer, A. Structure of Complex of Synthetic HIV-1 Protease with a Substrate-Based Inhibitor at 2.3 Å Resolution. *Science* **1989**, *246*, 1149−1152.

(33) Wlodawer, A.; Miller, M.; Jaskolski, M.; Sathyanarayana, B. K.; Baldwin, E.; Weber, I. T.; Selk, L. M.; Clawson, L.; Schneider, J.; Kent, S. B. H. Conserved Folding in Retroviral Proteases: Crystal Structure of a Synthetic HIV-1 Protease. *Science* **1989**, *245*, 616−621.

(34) Brik, A.; Wong, C.-H. HIV-1 Protease: Mechanism and Drug Discovery. *Org. Biomol. Chem.* **2003**, *1*, 5−14.

(35) Freidinger, R. M.; Veber, D. F.; Perlow, D. S.; Brooks, J. R.; Saperstein, R. Bioactive Conformation of Luteinizing-Hormone-Releasing Hormone: Evidence from a Conformationally Constrained Analog. *Science* **1980**, *210*, 656−658.

(36) Thaisrivongs, S.; Pals, D. T.; Turner, S. R.; Kroll, L. T. Conformationally Constrained Renin Inhibitory Peptides: γ-Lactam-Bridged Dipeptide Isostere as Conformational Restriction. *J. Med. Chem.* **1988**, *31*, 1369−1376.

(37) Robinson, B. S.; Riccardi, K. A.; Gong, Y.-F.; Guo, Q.; Stock, D. A.; Blair, W. S.; Terry, B. J.; Deminie, C. A.; Djang, F.; Colonno, R. J.; Lin, P.-F. BMS-232632, a Highly Potent Human Immunodeficiency Virus Protease Inhibitor That Can Be Used in Combination with Other Available Antiretroviral Agents. *Antimicrob. Agents Chemother.* **2000**, *44*, 2093−2099.

(38) Herrmann, J. L.; Schlessinger, R. H. Method for Alkylating Lactones. *J. Chem. Soc., Chem. Commun.* **1973**, 711−712.

(39) Maldaner, A. O.; Pilli, R. A. Stereoselective Alkylation of N-Boc-2-pyrrolidinones and N-Boc-2-piperidinones. Synthesis and Characterization of Disubstituted Lactams. *Tetrahedron* **1999**, *55*, 13321−13332.

(40) Johnson, T. A.; Jang, D. O.; Slafer, B. W.; Curtis, M. D.; Beak, P. Asymmetric Carbon−Carbon Bond Formations in Conjugate Additions of Lithiated N-Boc Allylic and Benzylic Amines to Nitroalkenes: Enantioselective Synthesis of Substituted Piperidines, Pyrrolidines, and Pyrimidinones. *J. Am. Chem. Soc.* **2002**, *124*, 11689−11698.

(41) Meyers, A. I.; Seefeld, M. A.; Lefker, B. A.; Blake, J. F. Origin of Stereochemistry in Simple Pyrrolidinone Enolate Alkylations. *J. Am. Chem. Soc.* **1997**, *119*, 4565−4566.

(42) Sprules, T. J.; Lavallee, J. F. Unexpected Contrasteric Alkylation Leading to a Model for 5-Membered Ring Enolate Alkylation: Short Stereoselective Synthesis of (±)-Acetomycin. *J. Org. Chem.* **1995**, *60*, 5041−5047.

(43) Orrling, K. M.; Wu, X. Y.; Russo, F.; Larhed, M. Fast, Acid-Free, and Selective Lactamization of Lactones in Ionic Liquids. *J. Org. Chem.* **2008**, *73*, 8627−8630.

(44) Welton, T.; Hallett, J. P. Room-Temperature Ionic Liquids: Solvents for Synthesis and Catalysis. 2. *Chem. Rev.* **2011**, *111*, 3508−3576.

(45) Rassu, G.; Zanardi, F.; Battistini, L.; Gaetani, E.; Casiraghi, G. Expeditious Syntheses of Sugar-Modified Nucleosides and Collections Thereof Exploiting Furan-, Pyrrole-, and Thiophene-Based Siloxy Dienes. *J. Med. Chem.* **1997**, *40*, 168−180.

(46) Boger, D. L.; Schule, G. Synthesis of Acyclic Precursors to (3*S*,4*S*)-4-Hydroxy-2,3,4,5-tetrahydro-pyridazine-3-carboxylic acid and Incorporation into a Luzopeptin/Quinoxapeptin Dipeptide. *J. Org. Chem.* **1998**, *63*, 6421−6424.

(47) Zienty, F. B.; Steahly, G. W. N-Substituted 2-Pyrrolidones. *J. Am. Chem. Soc.* **1947**, *69*, 715−716.

(48) Zawadzki, S.; Zwierzak, A. Simple Approach to 1-Alkyl-2-isopropylhydrazines. *Pol. J. Chem.* **2003**, *77*, 315−319.

(49) Freedman, H. H. Industrial Applications of Phase-Transfer Catalysis (Ptc): Past, Present and Future. *Pure Appl. Chem.* **1986**, *58*, 857−868.

(50) Wang, M. L.; Tseng, Y. H. Analysis of Phase-Transfer-Catalyzed O-Alkylation Reaction Using Fractional Factorial Design Method. *Chem. Eng. Commun.* **2005**, *192*, 557−574.

(51) Pappo, R.; Allen, D. S.; Lemieux, R. U.; Johnson, W. S. Osmium Tetroxide-Catalyzed Periodate Oxidation of Olefinic Bonds. *J. Org. Chem.* **1956**, *21*, 478−479.

(52) Panico, R.; Powell, W. H.; Richer, J. C. *A Guide to IUPAC Nomenclature of Organic Compounds: Recommendations 1993*, 1st ed.; Blackwell Scientific Publications: Oxford, U.K., 1993; 208 pp.

(53) See Supporting Information for illustrations where the stereochemistry is indicated for each molecule.

(54) Miyaura, N.; Suzuki, A. Palladium-Catalyzed Cross-Coupling Reactions of Organoboron Compounds. *Chem. Rev.* **1995**, *95*, 2457−2483.

(55) Larhed, M.; Hallberg, A. Microwave-Promoted Palladium-Catalyzed Coupling Reactions. *J. Org. Chem.* **1996**, *61*, 9582−9584.

(56) Larhed, M.; Moberg, C.; Hallberg, A. Microwave-Accelerated Homogeneous Catalysis in Organic Chemistry. *Acc. Chem. Res.* **2002**, *35*, 717−727.

(57) Kappe, C. O.; Dallinger, D. The Impact of Microwave Synthesis on Drug Discovery. *Nat. Rev. Drug Discovery* **2006**, *5*, 51−63.

(58) Brown, H. C.; Knights, E. F.; Scouten, C. G. Hydroboration XXXVI. Direct Route to 9-Borabicyclo[3.3.1]nonane via Cyclic Hydroboration of 1,5-Cyclooctadiene. 9-Borabicyclo[3.3.1]nonane as a Uniquely Selective Reagent for Hydroboration of Olefins. *J. Am. Chem. Soc.* **1974**, *96*, 7765−7770.

(59) Parikh, J. R.; Doering, W. V. E. Sulfur Trioxide in Oxidation of Alcohols by Dimethyl Sulfoxide. *J. Am. Chem. Soc.* **1967**, *89*, 5505−5507.

(60) Zhang, Q.; Jin, H.-X.; Wu, Y. A Facile Access to Bridged 1,2,4-Trioxanes. *Tetrahedron* **2006**, *62*, 11627−11634.

(61) Gronowitz, S.; Bjork, P.; Malm, J.; Hornfeldt, A. B. The Effect of Some Additives on the Stille Pd⁰-Catalyzed Cross-Coupling Reaction. *J. Organomet. Chem.* **1993**, *460*, 127−129.

(62) Flöistrup, E.; Goede, P.; Strömberg, R.; Malm, J. Synthesis of estradiol backbone mimics via the Stille reaction using copper(II) oxide as co-reagent. *Tetrahedron Lett.* **2011**, *52*, 209−211.

(63) Farina, V.; Kapadia, S.; Krishnan, B.; Wang, C. J.; Liebeskind, L. S. On the Nature of the Copper Effect in the Stille Cross-Coupling. *J. Org. Chem.* **1994**, *59*, 5905−5911.

(64) Wempe, M. F.; Anderson, P. L. Atazanavir Metabolism According to CYP3A5 Status: An in Vitro−in Vivo Assessment. *Drug Metab. Dispos.* **2011**, *39*, 522−527.

(65) Weber, I. T.; Agniswamy, J. HIV-1 Protease: Structural Perspectives on Drug Resistance. *Viruses* **2009**, *1*, 1110−1136.

(66) Navia, M. A.; Fitzgerald, P. M. D.; Mckeever, B. M.; Leu, C. T.; Heimbach, J. C.; Herber, W. K.; Sigal, I. S.; Darke, P. L.; Springer, J. P. Three-Dimensional Structure of Aspartyl Protease from Human Immunodeficiency Virus HIV-1. *Nature* **1989**, *337*, 615−620.

(67) Wlodawer, A.; Erickson, J. W. Structure-Based Inhibitors of HIV-1 Protease. *Annu. Rev. Biochem.* **1993**, *62*, 543−585.

(68) Bagossi, P.; Cheng, Y. S. E.; Oroszlan, S.; Tozser, J. Comparison of the Specificity of Homo- and Heterodimeric Linked HIV-1 and HIV-2 Proteinase Dimers. *Protein Eng.* **1998**, *11*, 439−445.

(69) Amat, M.; Lozano, O.; Escolano, C.; Molins, E.; Bosch, J. Enantioselective Synthesis of 3,3-Disubstituted Piperidine Derivatives by Enolate Dialkylation of Phenylglycinol-Derived Oxazolopiperidone Lactams. *J. Org. Chem.* **2007**, *72*, 4431−4439.

(70) Huang, A.; Kodanko, J. J.; Overman, L. E. Asymmetric Synthesis of Pyrrolidinoindolines. Application for the Practical Total Synthesis of (−)-Phenserine. *J. Am. Chem. Soc.* **2004**, *126*, 14043−14053.

(71) Otteneder, M.; Plastaras, J. P.; Marnett, L. J. Reaction of Malondialdehyde−DNA Adducts with Hydrazines: Development of a Facile Assay for Quantification of Malondialdehyde Equivalents in DNA. *Chem. Res. Toxicol.* **2002**, *15*, 312−318.